

ArchNURBS: NURBS-Based Tool for the Structural Safety Assessment of Masonry Arches in MATLAB[®]

Andrea Chiozzi¹; Marcello Malagù²; Antonio Tralli³; and Antonio Cazzani⁴

ABSTRACT

A new approach toward a fully CAD-integrated structural analysis of arched masonry structures is proposed and a new MATLAB[®]-based computational tool, named ArchNURBS, is developed. It is addressed to professionals dealing with restoration or structural rehabilitation of historical constructions, who need to assess the safety of masonry arches under assigned load distributions. By using it, they can easily produce estimates of the carrying capacity of curved masonry members, and specifically arches of arbitrary shape. A Computer Aided Design (CAD) environment, which is very popular among professionals, can be employed to provide a Non-Uniform Rational B-Splines (NURBS) representation of the arch geometry. On the basis of such a representation it is then possible to perform both an elastic isogeometric analysis and a limit analysis of the structure up to the collapse load. Moreover, the developed tool is also devised for handling the presence of Fiber-Reinforced Polymers (FRP) reinforcement strips at the extrados and/or the intrados. This allows for the design of properly dimensioned reinforcement and its verification according to current building codes. The entire procedure relies upon a sound theoretical background. ArchNURBS is going to be freely distributed as an open-source project (<http://sourceforge.net/projects/archnurbs/>).

Keywords: Masonry, Arches, Computer Aided Design, Elastic analysis, Limit analysis, Fiber

¹Corresponding Author, PhD, Postdoctoral Fellow, Department of Engineering, University of Ferrara, 1 Via Saragat, I-44122 Ferrara, Italy. E-mail: andrea.chiozzi@unife.it

²PhD Student, Department of Engineering, University of Ferrara, 1 Via Saragat, I-44122 Ferrara, Italy. E-mail: marcello.malagu@unife.it

³Full Professor, Department of Engineering, University of Ferrara, 1 Via Saragat, I-44122 Ferrara, Italy. E-mail: tra@unife.it

⁴Associate Professor, Department of Civil and Environmental Engineering and Architecture, University of Cagliari, 2 Via Marengo, I-09123 Cagliari, Italy. E-mail: antonio.cazzani@unica.it

21 reinforced polymers

22 **INTRODUCTION**

23 The paper is concerned with an ancient topic, the analysis of the structural behavior of curved
24 masonry members like arches, which is here being revisited through modern tools, leading to the
25 development of a new MATLAB[®]-based open-source computational tool named ArchNURBS for
26 the safety assessment of masonry arches.

27 Currently, there is a large amount of literature regarding the analysis up to collapse of masonry
28 arches and several methods are available for the assessment of the mechanical behaviour of his-
29 torical masonry constructions. The interested reader is addressed to (Roca et al. 2007) and (Tralli
30 et al. 2014) for an extensive state-of-the-art survey. A number of commercial software products
31 which allow evaluating the bearing capacity of a masonry arch have been developed (LimitState
32 Ltd. 2007; Gelfi 2008; AEDES 2014). However, these computer codes mainly cover those cases in
33 which the arch shape can be assimilated to a polyline. Nonetheless, even though many arches may
34 be correctly represented by a polyline, there is a wide class of arches which are not. For instance,
35 this is the case of either masonry arches where the dimensions of the blocks are much smaller than
36 the arch characteristic dimensions (see, for example, the three-centered masonry arch of Llanell-
37 tyd Bridge, Wales, portrayed in Fig. 1a) or arches composed by rounded stone voussoirs (see, for
38 example, the arch of Porta Asinaria in Rome, Italy, depicted in Fig. 1b). Furthermore, a suitable
39 approach capable of accurately and efficiently analyzing these cases is still lacking. Computer
40 Aided Design (CAD) is a natural environment for developing a tool for the analysis of masonry
41 arches which is both efficient and intuitive for professionals in the field of structural engineering
42 and structural rehabilitation of historical masonry constructions, among which the use of CAD
43 design representation techniques is widespread.

44 A CAD geometric representation of curved masonry members of arbitrary shape can be ob-
45 tained through the use of Non-Uniform Rational B-Splines (NURBS) which consist of rational
46 basis functions built upon common B-Splines basis functions in such a way that a given set of
47 points lying in a known range is suitably approximated with a sufficiently high degree of regu-

48 larity. Development of NURBS began in the 1950s and was carried out by engineers (mostly in
49 the car manufacturing business) who needed a mathematically precise representation of free-form
50 surfaces like those used for ship hulls, aerospace exterior surfaces, and car bodies, which could be
51 exactly reproduced whenever it was technically needed. NURBS are commonly used in Computer
52 Aided-Design (CAD), -Manufacturing (CAM), and -Engineering (CAE) systems and are part of
53 numerous industry-wide standards. They can be efficiently handled by computer programs and yet
54 allow for easy human interaction. In general, editing NURBS geometries is highly intuitive and
55 predictable. Moreover, NURBS exactly represent particular geometries such as circles, parabolas
56 and ellipses (Piegl and Tiller 1997).

57 In the last decade, NURBS have been extensively studied and developed for both describing
58 the geometry of a structural model and for representing (with the role of basis functions) the dis-
59 placement field within the Finite Element Method (FEM) (Hughes et al. 2005). Even if the use
60 of polynomial functions belonging to the spline family for the approximate solution of boundary
61 value problems dates back almost four decades (see e.g. (Prenter 1975; de Boor 1978; Benedetti
62 and Tralli 1989; Gontier and Vollmer 1995)) this new method, which is known as Iso-Geometric
63 Analysis (IGA), was precisely developed to cover the wide existing gap between the worlds of
64 FEM and CAD (see e.g. (Hughes et al. 2005; Bazilevs et al. 2006; Cottrell et al. 2009; Benson
65 et al. 2010; Auricchio et al. 2012)). As it is well-known, the term *isogeometric* is referred to a co-
66 incidence of the geometric model, which is built in a CAD environment, and the structural model
67 (i.e. the FEM model) used for performing stress analysis. In traditional FEM analysis structural
68 model and geometric model never coincide since they are both representations of a true object but
69 relying on different basis functions. This, in turn, produces accuracy-related issues in the com-
70 putations, particularly for curved thin structures. Besides, if NURBS are used as basis functions,
71 their smoothness is inherited by the FEM model, too: this is particularly important because it al-
72 lows circumventing some serious difficulties in developing finite elements, e.g. flexible beams and
73 plates where both bending and shear deformation must be accounted for. Moreover, the better a
74 function is approximated, the smaller the error affecting its derivatives: since stress fields are not

75 the primary solution variables, but need to be computed by differentiating displacements through
76 post-processing techniques, smoother displacement fields ensure a more accurate approximation
77 of the stresses.

78 On the other side, the growing interest in the preservation of masonry structures gave, in the
79 past, an impulse towards the development of new efficient tools for evaluating the ultimate load-
80 bearing capacity of these structures, in particular of masonry arches. From a mechanical point of
81 view, the analysis of masonry arches begins with the contributions of the late 1600s English school
82 (Hooke, Gregory) who stated the analogy between the inverted shape of a catenary and an arch
83 subjected to compressive stresses. Nowadays a sound theoretical framework for the evaluation of
84 masonry arches exists and it can be affirmed (following Huerta (Huerta 2001) and Como (Como
85 2013)) that the modern theory of limit analysis of masonry structures, which has been developed
86 mainly by Heyman (Heyman 1966; Heyman 1982), is a powerful tool for properly understanding
87 and analyzing curved masonry structures. Many other methods of analysis, other than limit anal-
88 ysis, can be used, of course, for determining the ultimate load carrying capacity of masonry arch
89 bridges, e.g. non-linear FEM analysis, discrete element analysis, hybrid discrete/finite element
90 methods etc. (see, for instance, (Crisfield 1997; Cundall and Strack 1979; Munjiza 2004)) and a
91 number of commercial FEM codes have been developed (e.g. DIANA). However, with such meth-
92 ods the collapse load is identified as a by-product of an indirect (and potentially long) iterative non
93 linear analysis procedure, which is often prone to numerical instabilities. Moreover, a non-linear
94 incremental analysis of a masonry structure requires the definition of many material parameters
95 which have to be precisely known in order to get reliable results. Finally, limit analysis may sim-
96 ply be extended to the case of masonry having a limited compressive strength (see e.g. (Livesley
97 1992; Orduna and Lourenço 2003)) and to the case of FRP (fiber-reinforced polymers) reinforced
98 arches (see e.g. (Caporale et al. 2006; Basilio et al. 2014; Briccoli Bati et al. 2013)).

99 Nevertheless, a NURBS-based approach to limit analysis is still lacking. Moreover, a software
100 product for the structural analysis of masonry arches which is capable of dealing with complex
101 geometries which are not adequately approximated by a polyline has not been devised yet. Such a

102 tool should allow the user to import the exact arch geometry, which can be easily generated within
103 a CAD environment using NURBS curves. In addition, the tool should allow the user to carry
104 out both an elastic and a limit analysis of the arch to be studied in order to assess its mechanical
105 response respectively under service loads and at failure. In order to reach a new level of accuracy
106 and to make the usage of the software simple and intuitive, such analyses should be based on the
107 NURBS representation of the arch geometry.

108 In this paper, a new open-source CAD-based tool for the analysis of masonry arches which
109 is specifically addressed to professionals in the field of structural engineering and structural re-
110 habilitation of historical masonry constructions is proposed. The tool, named ArchNURBS and
111 developed in MATLAB[®] environment, is based on a combination of IGA and limit analysis, both
112 relying on the NURBS representation of the arch which can be easily obtained from CAD design
113 products which are very popular among professional architects and civil engineers. As already
114 discussed, NURBS representation of the arch guarantees a higher accuracy of analysis, especially
115 when compared to a standard polyline representation of the same arch. An isogeometric finite ele-
116 ment elastic analysis of the arch can be useful to assess the response of the arch under usual service
117 loads which should not push the thrust line out of the arch depth. Even if standard curved finite ele-
118 ments could be used to accurately analyze an arbitrarily shaped arch, these tools are quite advanced
119 and often out-of-reach for a professional engineer or architect, whereas IGA allows for greater ac-
120 curacy without requiring the final user any particular effort. On the other hand, a NURBS-based
121 limit analysis is used for assessing the ultimate bearing capacity of the arch. Therefore, the pro-
122 posed tool allows for a fast evaluation of the safety level of a masonry arch under various loading
123 conditions. Furthermore, algorithms which allows to take into account the effect of masonry crush-
124 ing, sliding between blocks and additional FRP reinforcements placed either at the intrados or at
125 extrados of the arch have been devised and implemented.

126 Such a tool could be particularly appreciated if one considers, for instance, the widespread
127 damages that the 2012 Emilia (Italy) earthquake produced to ancient historical buildings, with a
128 great loss for the Italian cultural heritage; after the earthquake, professionals engineers and archi-

129 tects have been called to assess the safety of a huge number of ancient masonry constructions,
130 where arched and vaulted systems are recurrent, and to devise effective seismic retrofit interven-
131 tions. Another reason lies in the fact that since the exact shape of the arch to be studied is usually
132 not known in advance, a precise surveying of the structure is needed. This surveying is often
133 carried out through the use of laser scanning techniques which may be imported in a CAD envi-
134 ronment as a cloud of points. A CAD exact representation of the arch geometry is then possible
135 and constitutes the basis upon which both an elastic and a limit analysis can be performed in an
136 integrated way.

137 ArchNURBS is the first computational tool proposed in literature which allows for the eval-
138 uation of the load bearing capacity, and thus of the safety level, of arbitrarily loaded masonry
139 arched structures, starting from a NURBS representation of the real arch generated within a CAD
140 environment. To this aim, a new NURBS-based approach to limit analysis has been devised and
141 extensions which allows to include finite masonry compressive strength, sliding between blocks
142 and FRP reinforcement have been added to it. Finally, an isogeometric analysis has been made
143 possible within ArchNURBS in order to allow the user to evaluate the elastic structural response
144 of the arch under the action of service loads.

145 The paper is organized as follows: in Section 2 a synthetic survey on how the geometric shape
146 of a masonry arch can be described by a NURBS representation is given. The adopted struc-
147 tural models and isogeometric elastic analysis are then recalled and commented upon in Section 3.
148 In Section 4 we address the limit analysis based on the NURBS geometry representation of the
149 arch and its application to the case of FRP reinforced arches and to masonry arches with a lim-
150 ited compressive strength. Section 5 is devoted to presenting a comparison with experimental re-
151 sults taken from literature and some meaningful numerical examples, all of them developed within
152 ArchNURBS. Finally, conclusions will be drawn in Section 6.

153 **GEOMETRY DESCRIPTION**

154 ArchNURBS is a structural analysis tool for masonry arches having arbitrary shape based
155 on a NURBS representation of the arch geometry which can be easily obtained within a CAD

156 design environment. Description and computation of geometries in commercial CAD packages are
 157 based on B-splines and NURBS. More precisely, NURBS basis functions are built on B-splines
 158 basis functions which are piecewise polynomial functions defined by a sequence of coordinates
 159 $\Xi = \{\xi_1, \xi_2, \dots, \xi_{n+p+1}\}$, also known as the *knot vector*, where the so-called *knots* $\xi_i \in [0, 1]$ are
 160 points in a parametric domain whereas p and n denote the polynomial order and the total number
 161 of basis functions, respectively. The distance between two consecutive knots is named knot span
 162 and it represents the equivalent of the element domain in traditional finite elements. Once the order
 163 of the basis functions and the knot vector are known, the i -th B-spline basis function $N_{i,p}$ can be
 164 computed by means of the Cox-de Boor recursion formula (Cox 1972; de Boor 1978), which is not
 165 reported here for the sake of brevity.

166 As previously mentioned, B-splines are the starting point for the computation of the NURBS
 167 basis functions. Indeed, given a set of weights $w_i \in \mathbb{R}$, the NURBS basis functions $R_{i,p}$ read

$$168 \quad R_{i,p}(\xi) = \frac{N_{i,p}(\xi) w_i}{\sum_{i=1}^n N_{i,p}(\xi) w_i}. \quad (1)$$

169 NURBS share many properties with B-spline basis functions (Piegl and Tiller 1997). Among these,
 170 they are all non-negative, they have a compact support and build a partition of unity (PoU), that is

$$171 \quad \sum_{i=1}^n N_{i,p}(\xi) = \sum_{i=1}^n R_{i,p}(\xi) = 1 \quad (2)$$

172 for each $\xi \in [0, 1]$ (see (Hughes et al. 2005)). Hence, it is noteworthy from Eqs. (1) and (2)
 173 that B-spline basis functions can be thought of as NURBS basis functions when all weights w_i are
 174 equal to one. However, NURBS basis functions have the great advantage of representing exactly
 175 the geometry of a wide set of curves such as circles, ellipses and parabolas (Piegl and Tiller 1997)
 176 and of the surfaces which can be generated by them.

177 Geometries which can be represented with B-spline and NURBS are obtained as linear combi-
 178 nations of basis functions (Piegl and Tiller 1997; Farin 2002). For instance, if we consider a set of
 179 B-spline basis functions $N_{i,p}$ (the same holds for the NURBS basis functions) with $i = 1, \dots, n$,

180 it is possible to define a curve $\mathbf{C}(\xi) \in \mathbb{R}^d$ as

$$181 \quad \mathbf{C}(\xi) = \sum_{i=1}^n N_{i,p}(\xi) \mathbf{B}_i, \quad (3)$$

182 where coefficients $\mathbf{B}_i \in \mathbb{R}^d$ are known as control points (in the following, $d = 2$ is assumed since
183 this work focuses on planar curves). Differently from standard Lagrange and Hermite approxi-
184 mations, B-spline geometries do not usually interpolate these points. The continuity of the curve
185 follows from that of the adopted basis functions (Hughes et al. 2005) which, in general, is \mathcal{C}^{p-1}
186 throughout the domain. However, if a knot has multiplicity m , the continuity decreases m times at
187 that point (see (Piegl and Tiller 1997)).

188 Modeling CAD geometries inevitably involves several ingredients, such as knots, order of the
189 approximation and control points. However, in many practical applications only few of these
190 parameter are known *a priori*. In reverse engineering processes, for example, CAD models are
191 created by interpolating or approximating a set of points $\mathbf{P}_i \in \mathbb{R}^2$ usually obtained from the
192 real object by means of laser scanner records. Nonetheless, the parameterization of the input data
193 for B-spline and NURBS geometries addresses a crucial issue concerning the quality of the final
194 curve. Hence, there have been several attempts to improve the accuracy of B-spline and NURBS
195 approximations and interpolations (de Boor 1978; Hartley and Judd 1980; Lee 1989; Sarkar and
196 Menq 1991; Farin 2002). In particular, some of these parameterization techniques, such as the
197 uniform method, the arch-length method and the centripetal method are available in several CAD
198 programs (Autodesk, Inc. 2007).

199 The easiest way to assess the quality of the computed curve is to evaluate the distance between
200 the CAD geometry $\mathbf{C}(\xi)$ and the analytical representation of the real curve $\mathbf{F}(\xi)$. Therefore, the
201 distance between these two curves at the parametric point ξ is calculated as

$$202 \quad d(\xi) = \min_{\xi} \{ |\mathbf{C}(t) - \mathbf{F}(\xi)| \}. \quad (4)$$

203 Once the value of $d(\xi)$ has been evaluated for n given data points, the errors in the L_∞ norm may

204 be defined:

$$205 \quad E_\infty = \max_{i=1}^n \{d_n\}, \quad (5)$$

206 and in the L_2 norm:

$$207 \quad E_2 = \left[\frac{1}{n} \sum_{i=1}^n d_n^2 \right]^2. \quad (6)$$

208 Thus, for the sake of completeness we investigate the quality of the NURBS curve reported in
209 Figure 2 in approximating a three-centered (or polycentric) arch composed of three circular arcs
210 jointed together with \mathcal{C}^1 continuity. The radius R_i and the center of each portion are also shown.
211 The NURBS curve has been drawn in AutoCAD[®] 2013 by interpolating the set of points P_i
212 indicated by red circles in Figure 2 with cubic NURBS basis functions. In particular, the position
213 of these points has been calculated by dividing each of the three circular arcs in equal parts. Table 1
214 summarizes both the maximum (i.e. E_∞) and the mean (E_2) errors obtained by approximating the
215 exact geometry of the polycentric arch with its polyline and NURBS representations. As it is
216 expected, the error decreases with the number of interpolating points and NURBS representation
217 proves more accurate.

218 **LINEAR ELASTIC ANALYSIS**

219 As previously stated, a linear elastic analysis of a masonry arch may still be meaningful for
220 several arches undergoing service loads, which usually are considerably lower than collapse loads
221 and might not push the thrust line out of the shape of the arch. ArchNURBS allows for an elastic
222 isogeometric analysis (IGA) of the masonry arch under study, based on its NURBS representation.
223 In this Section an introduction to the IGA of a plane curved Timoshenko beam (Cazzani et al.
224 2014c) is given. Interesting studies on IGA of curved rods (even though Kirchhoff-Love rods) in
225 the three dimensional space may be found in (Greco and Cuomo 2013; Greco and Cuomo 2014).
226 In addition, some recent investigations of the application of IGA for the analysis of strongly curved
227 beams are contained in (Cazzani et al. 2014b; Cazzani et al. 2014a).

228 As it is depicted in Figure 3, we consider a Cartesian reference system $O(x, y)$ and a local
229 reference system $O'(t', n')$ where t' and n' are the unit-tangent and the unit-normal vectors to the

230 beam axis. Further, we introduce the curvilinear abscissa $s \in [0, l]$ which spans the centroidal line
 231 of the plane curved beam, whose length is l , is defined by the parametric representation

$$232 \quad \begin{cases} x(s) = \sum_{i=1}^n N_{i,p}(s(\xi)) x_i & \text{and} \\ y(s) = \sum_{i=1}^n N_{i,p}(s(\xi)) y_i \end{cases} \quad (7)$$

233 where x_i and y_i are the control points coordinates. Thus, the unit tangent and normal vectors of a
 234 NURBS curve at a parametric point s are calculated as (Lipshultz 1969)

$$235 \quad t' = \frac{(x_{,s}, y_{,s})}{\sqrt{x_{,s}^2 + y_{,s}^2}} \quad (8)$$

236 and

$$237 \quad n' = (y_{,s}, -x_{,s}) \cdot \frac{x_{,ss}y_{,s} - x_{,s}y_{,ss}}{(x_{,s}^2 + y_{,s}^2)^2} \quad (9)$$

238 where comma denotes differentiation. Further, the curvature radius reads

$$239 \quad R(s) = \frac{(x_{,s}^2 + y_{,s}^2)^{3/2}}{|x_{,s}y_{,ss} - x_{,ss}y_{,s}|}. \quad (10)$$

240 In order to describe the kinematics of a curved Timoshenko beam we consider the displacement
 241 and the load vectors

$$242 \quad \mathbf{u} = [u, v, \phi]^T \quad \text{and} \quad \mathbf{p} = [q_t, q_r, m]^T, \quad (11)$$

243 referred to the local reference system (where $(\cdot)^T$ denotes the transpose). In particular, u and v are
 244 the tangential and normal displacement of the cross-section centroid, ϕ the cross-section rotation,
 245 q_t and q_r the tangential and radial distributed loads and m the distributed bending couples. Hence,
 246 by assuming small deformations, the equilibrium, compatibility and constitutive equations for the

247 plane-curved Timoshenko beam are

$$248 \quad N_{,s} - \frac{T}{R} + q_t = 0, \quad T_{,s} + \frac{N}{R} + q_r = 0 \quad \text{and} \quad M_{,s} - T + m = 0, \quad (12)$$

$$249 \quad \varepsilon = u_{,s} - \frac{v}{R}, \quad \gamma = v_{,s} + \frac{u}{R} + \phi \quad \text{and} \quad \chi = \phi_{,s}, \quad (13)$$

$$251 \quad N = EA\varepsilon, \quad T = GAk_s\gamma \quad \text{and} \quad M = EJ\chi, \quad (14)$$

253 where the generalized stresses N , T and M denote the axial force, the shear force and the bending
 254 moment, whereas the generalized strains ε , γ and χ are the axial, the shear and the curvature
 255 deformations. Finally, symbols E , G , A , J and k_s are respectively the Young's modulus, the shear
 256 modulus, the cross sectional area, the area moment of inertia and the shear-correction factor.

257 The first step towards a finite element solution of the problem is represented by the definition
 258 of the total potential energy of the system

$$259 \quad \Pi = \frac{1}{2} \int_0^l (EA\varepsilon^2 + GAk_s\gamma^2 + EJ\chi^2) \, ds - \int_0^l (q_t u + q_r v + m\phi) \, ds. \quad (15)$$

260 Subsequently, by making use of the iso-parametric formulation, the discrete displacement field
 261 $\mathbf{u}^h(\xi) \in \mathbb{R}^2$ is defined as

$$262 \quad \mathbf{u}^h(\xi) = \sum_{i=1}^n N_{i,p}(\xi) \mathbf{u}_i, \quad (16)$$

263 where $\mathbf{u}_i = [u_i, v_i, \phi_i]$ are the displacements at the control points \mathbf{B}_i . It is worth noticing that,
 264 according to Eq. (3), the displacement field in Eq. (16) has been discretized with B-spline basis
 265 functions. Nonetheless, NURBS basis functions might have been used in cases where a NURBS-
 266 described curve is given. Hence, by making use of Eqs. (15) and (16) the discrete solution of the
 267 problem is defined as:

$$268 \quad \arg \min_{u, v, \phi} \left\{ \sum_{e=1}^{n_e} \left[\frac{1}{2} \int_{\xi_e}^{\xi_{e+1}} \left[EA (\varepsilon^h)^2 + GAk_s (\gamma^h)^2 + EJ (\chi^h)^2 \right] ds - \int_{\xi_e}^{\xi_{e+1}} \mathbf{p}^T \mathbf{u}^h ds \right] \right\}, \quad (17)$$

269 where n_e is the number of spans whereas ξ_e and ξ_{e+1} are the knots which correspond to the e -th

270 span. Once the numerical solution \mathbf{u}^h is known, the generalized stresses and strains are calculated
271 by means of Eqs. (13) and (14). Therefore, N , T and M and ε , γ and χ are defined with the
272 same NURBS basis functions used for approximating the displacement field \mathbf{u}^h . Accordingly, the
273 computation of the thrust line, which descends from the ratio M/N , is straightforward.

274 As in standard finite element discretizations, the numerical solution can be improved by refin-
275 ing the approximation. In particular, in IGA there are three different refinement techniques. The
276 first two are knot insertion (h -refinement) and polynomial order elevation (p -refinement) which
277 do not alter the geometry and the continuity of the curve. The third method, which is known as
278 k -refinement, consists in order elevation of the basis functions and consequent knots insertion.
279 This increases the continuity of the approximation without changing the geometry (Hughes et al.
280 2005; Cottrel et al. 2007). In ArchNURBS each of these methods may be used.

281 **LIMIT ANALYSIS**

282 As already discussed, limit analysis is a powerful tool to assess the structural safety level of a
283 masonry construction. It is well established that when *mechanism* and *equilibrium* formulations of
284 limit analysis are linearized, they produce dual Linear Programming (LP) problems (Charnes and
285 Greenberg 1951). In particular Livesley (Livesley 1978) has shown that the *equilibrium* formula-
286 tion can be applied to masonry arches. It involves the discretization of the arch into a number of
287 rigid blocks. Many researchers have developed procedures to model masonry arches as discrete
288 rigid blocks: among them we recall (Delbecq 1980; Boothby 1994; Gilbert and Melbourne 1994).

289 In ArchNURBS a joint equilibrium formulation, similar to that originally adopted by Lives-
290 ley (Livesley 1978) and then proposed for masonry arches in (Gilbert 2007) is used. It should be
291 incidentally observed that, while an equilibrium formulation has been formally used, assuming a
292 finite number of blocks (and hence of interfaces) provides actually an upper bound estimate of the
293 collapse multiplier.

294 The adopted model relies on the following traditional assumptions, originally proposed by
295 Heyman (see (Heyman 1969)) for the limit analysis of masonry arches:

- 296 1. sliding failure of adjacent units in the arch cannot occur;
- 297 2. masonry has zero tensile strength;
- 298 3. masonry has infinite compressive strength.

299 Therefore, a procedure based on an *equilibrium formulation* and the above assumptions for the
 300 limit analysis of masonry arches is set out as follows.

301 The structure is divided into c elements (blocks) in much the same way as for elastic analysis.
 302 Subsequently to this subdivision, $d = c + 1$ interfaces are generated. For each block the equations
 303 of equilibrium are written, in such a way as to express contact forces $\mathbf{q} = [T_i, N_i, M_i]$ (which
 304 are respectively the shear force, the axial force and the bending moment) acting on the i -th inter-
 305 element boundary and any external load acting on the element \mathbf{f} , which can be either a dead load
 306 \mathbf{f}_D or a live load $\lambda \mathbf{f}_L$. Such equations may be expressed as:

$$307 \quad \mathbf{A}\mathbf{q} - \lambda \mathbf{f}_L = \mathbf{f}_D, \quad (18)$$

308 where \mathbf{A} is a suitable $(3c \times 3d)$ equilibrium matrix containing the direction cosines of the unit-
 309 normal vector n' of the transversal section at each contact interface. These equations are the equi-
 310 librium constraints of the problem.

311 Yield constraints, in the no-tension material hypothesis, are then defined on \mathbf{q} :

$$312 \quad \left. \begin{array}{l} M_i \leq 0.5N_it_i \\ M_i \geq -0.5N_it_i \end{array} \right\} \forall \text{ contact } i = 1, \dots, c, \quad (19)$$

313 where t_i is the depth of the arch section at contact i . Finally the limit analysis problem for pro-
 314 portional loading is now written as *Maximize the load factor λ , subject to the equilibrium con-*
 315 *straints (18) and to the yield constraints (19):*

$$316 \quad \max\{\lambda\}. \quad (20)$$

317 Using this formulation the LP problem variables are the contact forces $(T_1, N_1, M_1, \dots, T_c, N_c, M_c)$
 318 and the unknown load factor λ . In ArchNURBS the linear programming problem is solved through
 319 the MATLAB[®] function `linprog.m` which is part of the MATLAB[®] Optimization Toolbox.

320 The yield constraints expressed in eq. (19) are valid only if the material exhibits an unlimited
 321 compressive strength. If, instead, it is assumed that masonry has a limited (i.e. finite) compressive
 322 strength σ_{crush} , and that thrust is transmitted, from one block to the next one, through a rectangular
 323 crush block, then, as it is suggested in (LimitState Ltd. 2011), Eq. (19) may be replaced by:

$$324 \left. \begin{aligned} M_i &\leq N_i \left(0.5t_i - \frac{N_i}{2\sigma_{\text{crush}} b} \right) \\ M_i &\geq -N_i \left(0.5t_i - \frac{N_i}{2\sigma_{\text{crush}} b} \right) \end{aligned} \right\} \forall \text{ contact } i = 1, \dots, c, \quad (21)$$

325 where σ_{crush} is the masonry compressive strength and b is the width of the arch transversal section.
 326 However, the constraints in Eq. (21) are non-linear. Therefore, in order to continue using a Linear
 327 Programming (LP) solver, these constraints need to be approximated by a set of linear constraints
 328 (see e.g. (Gilbert 2007; LimitState Ltd. 2011)).

329 In order to minimize the number of constraints in the problem (and to maximize computational
 330 efficiency) an iterative solution algorithm which involves only refining the representation of the
 331 failure envelope where required is used. The algorithm can be summarized in the following steps:

- 332 1. Initially solve the global LP problem with the original linear constraints (19) plus the addi-
 333 tional linear constraint $N_i < N_{i,max}$ on each contact i , where $N_{i,max}$ is the maximum axial
 334 force which the arch section can resist to before crushing occurs;
- 335 2. Substitute N_i from the last solution into the inequality constraints, eqs. (21), for each con-
 336 tact i . If a constraint is violated, calculate the violation factor e_i , i.e.

$$337 e_i = \frac{|M_i|}{N_i \left(0.5t_i - \frac{N_i}{2\sigma_{\text{crush}} b} \right)}, \quad (22)$$

338 and store, from the previous solution, the values of axial force corresponding to contacts

- 339 where violation has occurred. These values are denoted by $N_{i,0}$;
- 340 3. For each contact with $e_i \geq 1.0$ (i.e. such that violation occurs) set an additional linear
- 341 constraint which is tangential to the original failure envelope described by eqs. (21) at the
- 342 point corresponding to $N = N_{i,0}$;
- 343 4. Solve the new global LP problem;
- 344 5. Repeat from step 2 until the maximum value of $e_i < 1 + tol$ where the tolerance tol is taken
- 345 as a suitably small value.

346 Moreover, if sliding between blocks has to be taken into account, additional sliding yield con-

347 straints to the linear programming problem (20) are needed. As suggested in (Melbourne and

348 Gilbert 1995), it is possible to assume a simple associative friction model defining the following

349 *linear constraints*:

$$\left. \begin{array}{l} T_i \leq \mu_i N_i \\ T_i \geq -\mu_i N_i \end{array} \right\} \forall \text{ contact } i = 1, \dots, c, \quad (23)$$

351 where μ_i is a suitable friction coefficient for each contact interface i . This particular friction

352 model has been chosen for simplicity reasons whereas in literature more advanced models exist,

353 which involve non-associative friction laws and the use of both non-linear programming methods

354 (see e.g. (Ferris and Tin-Loi 2001; Orduna and Lourenço 2003)) and iterative linear-programming

355 methods (Gilbert et al. 2006). Nevertheless, applying the iterative procedure devised in (Gilbert

356 et al. 2006) to brickwork masonry arch bridges analyzed previously with an associative friction

357 model, (Gilbert and Ahmed 2004) found that the non-associative bridge strength predictions were

358 at most 6 percent lower, largely justifying the initial associative friction assumption.

359 For the sake of simplicity, backfill (which is considered as a dead load and thus enters in

360 Eq. (18)) is modeled as an external vertical force acting upon each block; it is given by the weight

361 of the volume of the backfill portion lying above each block and is applied to the center of mass

362 of the same volume. As discussed in (Callaway et al. 2012), it is necessary to point out that

363 the influence of the backfill on the load capacity of masonry arches is a very complex topic. In

364 literature, much more sophisticated models for backfill exist, which are capable of taking into

365 account effects like load diffusion and the gradual build-up of passive pressures (see e.g. (Gilbert
366 et al. 2007; Cavicchi and Gambarotta 2005)).

367 Finally, it is possible to modify the limit analysis in order to take into account the presence
368 of Carbon Fiber Reinforced Polymer (CFRP) reinforcement strips at the intrados and/or at the
369 extrados of the arch. Many researchers have proposed different solutions to this problem (see,
370 e.g. (Briccoli Bati et al. 2013; Basilio et al. 2014; Caporale et al. 2006; Caporale and Luciano
371 2012; Caporale et al. 2014)). In the present paper we deal with the problem by modifying the
372 original equilibrium formulation including two further variables $(F_{i,\text{intrados}}, F_{i,\text{extrados}})$ for each of the
373 n CFRP reinforced interfaces. These variables represent the inner force acting within the FRP
374 strip at the interface at the intrados and at the extrados respectively and enter into the equilibrium
375 constraints (18). The new variables are subjected to the *additional yield constraints*:

$$376 \left. \begin{array}{l} 0 < F_{i,\text{intrados}} < F_d \\ 0 < F_{i,\text{extrados}} < F_d \end{array} \right\} \forall \text{ reinforced contact } i = 1, \dots, n, \quad (24)$$

377 where F_d is the design delamination resistance of the CFRP strip which may be evaluated, for
378 example, following the prescriptions contained in Chapter 5 of (CNR2013).

379 NUMERICAL EXAMPLES

380 In this section a comparison with experimental results taken from literature and three numerical
381 examples analyzed with the computational tool ArchNURBS are presented. The comparison with
382 experimental results allows to validate the numerical results obtained with ArchNURBS. Further-
383 more, the influence of the geometric representation of the rigid blocks in which the arch is sub-
384 divided on the limit load multiplier λ is discussed. Then, the limit analysis for the three-centered
385 arch described in Section 2 and a *real world* arch are taken into consideration in the second and
386 third example, respectively.

387 **Comparison with experimental results**

388 In order to validate the results obtained with ArchNURBS a comparison with the experimen-
389 tal tests presented in (Vermeltoort 2001) and later analyzed in (Milani et al. 2008) is carried
390 out. (Vermeltoort 2001) tested the ultimate strength of a segmental masonry arch with a clear span
391 of 3 m, an inner radius of 2.5 m and a sagitta of 0.5 m. The arch is a one-head brick structure with
392 depth equal to 0.10 m and width equal to 1.25 m. The test-arch had 51 layers and was built with
393 Rijswaard soft mud bricks and 1:2:9 mortar. Brick compressive strength was 27 MPa and mortar
394 compressive strength was 2.5 MPa. The test-arch was loaded with four concentrated loads, applied
395 by four hydraulic jacks 600 mm centre to centre. In Fig. 4 the geometry of the test-arch and its
396 loading conditions are reported. Only the second concentrated load from the left was increased
397 until failure, whereas the remaining loads were maintained constant at the values of 5.9, 9.1 and
398 9.1 kN respectively. At failure, (Vermeltoort 2001) observed a four hinges collapse mechanism
399 which is depicted in Fig. 5a and measured a collapse load equal to 40.7 kN at the second jack.

400 The described test-arch has been modeled within ArchNURBS as a segmental arch formed
401 by 51 blocks and the same point loads used by (Vermeltoort 2001) in the experiments have been
402 applied. Only the second point load from the left have been marked as a live load. After a limit
403 analysis of the arch, ArchNURBS gives out a collapse value of 40.7 kN for the live load previously
404 defined. Thus, the value of the collapse load calculated by ArchNURBS coincides with the col-
405 lapse load measured during the experiments. Furthermore, a four hinges collapse mechanism has
406 been numerically determined. Fig. 5b depicts the collapse mechanism numerically computed with
407 ArchNURBS. The failure mechanism predicted by ArchNURBS is very close to the real failure
408 mechanism experimentally observed by (Vermeltoort 2001) when bringing to failure the test-arch.
409 Thus, it can be concluded that ArchNURBS gives an accurate prediction of both collapse load and
410 collapse mechanism of the masonry arch under study.

411 **Influence of the voussoirs geometry**

412 Many arches in the real-world occurrences are made of stone voussoirs which have a rounded
413 shape rather than a quadrangular shape, as shown for example in Fig. 1b, representing the arch of

414 Porta Asinaria in Rome (Italy). When the size of these voussoirs is not small their exact geometric
415 representation is of paramount importance in order to obtain accurate estimates of the collapse load
416 multiplier λ .

417 `ArchNURBS` allows for an exact description of the arch rounded voussoirs by exploiting the
418 features of NURBS geometries generated in CAD environments. On the contrary, most of existing
419 commercial software codes approximate the shape of rounded voussoirs with simple quadrangular
420 blocks.

421 In the case of a uniform vertical live load distribution, if the section depth of the arch is large
422 enough (as is, for example, in the arch of Fig 1b) and unless taking into account finite stone
423 compressive strength, the arch may result safe for every value of the applied load (Heyman 1969).

424 Nevertheless, let us consider a semi-circular arch with mean radius 2.125 m, section depth
425 0.250 m and width 0.500 m, loaded with a uniformly distributed vertical live load of 1 kN/m. In
426 this case, section depth is not great enough to guarantee the safety of the arch for every value of the
427 uniform vertical applied live load and a collapse load multiplier can be determined. The backfill
428 height is assumed equal to 3.00 m. The arch is subdivided into ten voussoirs. Material properties
429 of the stone-voussoirs and of the backfill are reported in Table 2.

430 `ArchNURBS`, which implements the limit analysis algorithms described in the previous Sec-
431 tion, returns a collapse load multiplier $\lambda = 9.8$ for the arch model with rounded voussoirs. The
432 obtained value is the exact collapse load multiplier for the rounded voussoirs arch here taken into
433 consideration.

434 On the other hand, if the arch is modeled by means of ten quadrangular voussoirs a collapse
435 load multiplier $\lambda = 8.9$ is computed (this result has been carried out with the commercial soft-
436 ware `LimitState:RING 3.0`[®]). Therefore, the geometrical approximation of the rigid blocks with
437 quadrangular elements leads to an error of 9.2 % on the estimate of λ .

438 Of course, the error could be greatly reduced if an higher number of quadrangular blocks was
439 chosen to model the arch but then the number of interfaces between blocks (on which hinges
440 positions are constrained to be) would be changed in respect to the original problem. In addition,

441 computational efficiency would be clearly reduced.

442 In Figures 6b-c a comparison between the two arch models is shown along with a plot of the
443 corresponding thrust line.

444 **Three-centered arch**

445 As shown in Fig. 1a, three-centered arches are recurrent in many masonry structures. The
446 three-centered arch described in Section 2 is examined, as an example, in this Subsection. In
447 particular, its depth and width are assumed equal to 0.560 m and 0.500 m, respectively. The exact
448 arch geometry has been generated within a CAD environment using NURBS curves and then
449 imported in ArchNURBS. Material properties used for masonry and for the backfill are reported
450 in Table 2. The masonry mechanical properties chosen are typical for low quality masonry as
451 suggested in the explicative circular (CIRC2009) related to the Italian Building Code (NTC2008
452).

453 The arch is supposed to be loaded by a downward linear uniform live load of 1 kN/m. This load
454 is amplified by a load multiplier λ . The arch has been subdivided into 90 rigid blocks. First, limit
455 analysis is performed without considering any backfill. In this case the collapse load multiplier is
456 $\lambda = 0.78$. As it is illustrated in Figure 7a the resulting collapse mechanism is a symmetrical five
457 hinges mechanism. The corresponding thrust line and position of hinges at collapse is indicated by
458 a red line and red circles, respectively. A collapse load multiplier less than 1 indicates that the arch,
459 in this configuration, is not safe under the action of the assigned linear uniform load of 1 kN/m.

460 The same analysis has been then carried considering a backfill having a height of 4.00 m and a
461 specific weight as indicated in Table 2. In this case, despite the collapse mechanism and the posi-
462 tion of the collapse thrust line being similar to those obtained in the previous case (see Figure 7b),
463 the load multiplier increases to $\lambda = 21.62$. Therefore, the particular geometry of the arch studied
464 in this example is very sensitive to the stabilizing effect of the backfill.

465 **A masonry arch from *Torre Fornasini***

466 The third arch here analyzed is a real world masonry arch belonging to the groin vault which
467 bears the first story of *Torre Fornasini*, a historical masonry tower construction in Poggio Renatico

468 (Italy), which was severely damaged by the earthquake which struck Emilia on May 2012. The
469 tower, depicted in Figure 8, has been subjected to extensive seismic retrofit intervention which
470 comprised reinforcement of the extrados of the vault with Carbon Fiber Reinforced Polymers
471 (CFRP) strips (Milani et al. 2014). In particular, the analyzed arch is the segmental arch shown
472 in Figure 9a. It is characterized by a span equal to 4.13 m, a midspan rise equal to 1.81 m, a
473 depth equal to 0.14 m and a width equal to 0.25 m. After an accurate survey, the exact arch ge-
474 ometry has been generated within a CAD environment using NURBS curves and then imported in
475 ArchNURBS. Again, material properties assumed for masonry and specific weight for the backfill
476 are reported in Table 2. The arch is loaded by a downward acting linear uniform live load equal
477 to 1 kN/m multiplied by a load multiplier λ . The arch has been subdivided into 90 rigid blocks.
478 First, limit analysis is performed without taking into account any backfill. In this case a solution
479 cannot be determined since the arch is not stable under its own weight. Then, the same analysis
480 is carried out by considering a backfill with specific weight reported in Table 2 and a maximum
481 height equal to 2.15 m. Under these assumptions, the optimization problem can be solved and
482 the resulting collapse mechanism is a symmetrical five-hinges mechanism which is depicted in
483 Figure 9b. The collapse load multiplier is $\lambda = 1.43$. In order to evaluate the effect of the limited
484 compressive strength of masonry on the load capacity of the structure the same limit analysis has
485 been carried out, allowing for a masonry compressive strength equal to 2.4 MPa, as indicated in
486 Table 2 and as prescribed by the explicative circular (CIRC2009) related to the Italian Building
487 Code (NTC2008), following the algorithm described in Section 4. In this case the collapse load
488 multiplier drops to $\lambda = 0.86$. As it has been explained in the previous Section it is also possible
489 to account for the effect of FRP reinforcement. Indeed, during the seismic retrofit intervention a
490 200 mm wide strip of carbon fiber tissue (MapeWrap C Uni-AX produced by MAPEI) was ap-
491 plied to the extrados of the vault. This tissue has thickness of 0.2 mm, Young's elastic modulus
492 of 230 GPa (for tensile stress only) and ultimate strain of 2%. FRP delamination force has been
493 calculated by following the Italian FRP Design Guidelines (CNR2013). By performing a limit
494 analysis of the FRP reinforced arch, without taking into account the effect of limited compressive

495 strength of masonry, the collapse load multiplier results $\lambda = 5.94$. In Figure 9c the symmetric five
496 hinges collapse mechanism is shown: in this case the mechanism which develops only after FRP
497 delamination has occurred at both sides of the arch. On the other hand, when the effect of finite
498 compressive masonry strength is considered and coupled to the FRP reinforcement, the collapse
499 load multiplier drops to $\lambda = 3.44$. In both cases FRP reinforcement is proven to be very effec-
500 tive in enhancing the safety level of the arch under study. Finally, an analysis of the original arch
501 without reinforcement has been considered by accounting for possible sliding of masonry blocks
502 as explained in Section 4. Therefore, after performing this limit analysis it can be observed that
503 adopting a friction coefficient $\mu = 0.3$, as it is widely suggested in literature (see e.g. (Vasconcelos
504 and Lourenço 2006)), the original solution does not change: collapse still occurs by formation of a
505 five hinges mechanism and the collapse multiplier is still $\lambda = 1.43$. Besides, if the friction coeffi-
506 cient is reduced to $\mu = 0.275$ it is observed that collapse mechanism modifies since sliding occurs
507 at the arch imposts. In this last case the collapse multiplier is $\lambda = 1.02$ and the corresponding
508 collapse mechanism and collapsed thrust line at collapse are shown in Figure 9d. Results from the
509 discussed analysis are summarized in Table 3.

510 CONCLUSIONS

511 This work introduced a new simple CAD-integrated computational tool for the safety assess-
512 ment of masonry arches addressed to professionals in the field of structural rehabilitation of his-
513 torical masonry constructions which cannot or do not want to get involved into more advanced
514 and demanding computational methods. The proposed software, named ArchNURBS, provides
515 a simple and very intuitive instrument for the accurate evaluation of the load bearing capacity of
516 masonry arches. ArchNURBS has been implemented in MATLAB[®] and is freely available online
517 at the address <http://sourceforge.net/projects/archnurbs/> as an open-source
518 project.

519 ArchNURBS is the first computational tool for the analysis of masonry arches proposed in
520 literature which is based on a NURBS description of the shape of the arch. Such representation
521 can be easily generated in a CAD environment which is very popular among professional engineers

522 and architects, possibly starting from topographical surveying data. NURBS representation allows
523 for an exact shape description of the arch, which is especially useful for those arch shapes which
524 are not well represented by a polyline. On the basis of such geometric representation, a preliminary
525 isogeometric finite element elastic analysis (useful to determine the response under service loads
526 which might not push the thrust line out of the shape of the arch) and a NURBS-based limit analysis
527 of the masonry arch (which is needed to assess the safety level of the structure) are possible.
528 Furthermore, limited compressive strength for masonry, sliding between blocks and presence of
529 FRP reinforcement can be dealt with in ArchNURBS.

530 A comparison with experimental results has shown that ArchNURBS can predict with great ac-
531 curacy the ultimate bearing capacity of masonry arches. In addition, some meaningful examples of
532 NURBS-based limit analysis of masonry arches obtained with ArchNURBS have been presented.

533 The new approach on which ArchNURBS is based has proved to be effective in providing an
534 accurate evaluation of the safety level of masonry arches of arbitrary shape, while requiring the
535 professional user little effort compared to existing computational techniques.

536 **ACKNOWLEDGEMENTS**

537 The financial support of RAS, the Autonomous Region of Sardinia, under grant number
538 F71J09999350002-CRP1 475 (Legge Regionale 7/2007, bando 2008, Progetto MISC: Metodi Iso-
539 geometrici per Strutture Curve) is gratefully acknowledged by M. Malagù and by Prof. A. M.
540 Cazzani. The researchers of the University of Ferrara gratefully acknowledge the financial support
541 of ReLUI3 programs WP2 (Analysis of the seismic response of masonry structures) and Task 2.2
542 (Horizontal structures, vaults, floors, roofs and their interaction with masonry structures).

REFERENCES

- AEDES (2014). “SAV, Stabilità di archi e volte in muratura, <<http://www.aedes.it>>.
- Auricchio, F., Beirão da Veiga, L., Hughes, T. J. R., Reali, A., and Sangalli, G. (2012). “Iso-geometric collocation for elastostatics and explicit dynamics.” *Computer Methods in Applied Mechanics and Engineering*, 249–252, 2–14.
- Autodesk, Inc. (2007). *Autodesk[®] MAYA[®] 8.5 - NURBS modeling*.
- Basilio, I., Fedele, R., Lourenço, P., and Milani, G. (2014). “Assessment of curved FRP-reinforced masonry prisms: experiments and modeling.” *Construction and Building Materials*, 51, 492–505.
- Bazilevs, Y., Calo, V. M., Zhang, Y., and Hughes, T. J. R. (2006). “Isogeometric fluid-structure interaction analysis with applications to arterial blood flow.” *Computational Mechanics*, 38, 310–322.
- Benedetti, A. and Tralli, A. (1989). “A new hybrid F.E. model for Arbitrarily curved beam. I — Linear analysis.” *Computers and Structures*, 33(6), 1437–1449.
- Benson, D. J., Bazilevs, Y., Hsu, M. C., and Hughes, T. (2010). “Isogeometric shell analysis: the Reissner-Mindlin shell.” *Computer Methods in Applied Mechanics and Engineering*, 199, 276–289.
- Boothby, T. E. (1994). “Stability of masonry piers and arches including sliding.” *ASCE Journal of Engineering Mechanics*, 120, 304–319.
- Briccoli Bati, S., Fagone, M., and Rotunno, T. (2013). “Lower bound limit analysis of masonry arches with CFRP Reinforcements: a numerical method.” *Journal of Composites for Construction*, 17, 543–553.
- Callaway, P., Gilbert, M., and Smith, C. (2012). “Influence of backfill on the capacity of masonry arch bridges.” *Proceedings of the Institution of Civil Engineers: Bridge Engineering*, 165, 147–157.
- Caporale, A., Feo, L., Hui, D., and Luciano, R. (2014). “Debonding of FRP in multi-span masonry arch structures via limit analysis.” *Composite Structures*, 108, 856–865.

570 Caporale, A. and Luciano, R. (2012). “Limit analysis of masonry arches with finite compres-
571 sive strength and externally bonded reinforcement.” *Composites Part B: Engineering*, 43,
572 3131–3145.

573 Caporale, A., Luciano, R., and Rosati, L. (2006). “Limit analysis of masonry arches with externally
574 bonded FRP reinforcements.” *Computer Methods in Applied Mechanics and Engineering*, 196,
575 247–260.

576 Cavicchi, A. and Gambarotta, L. (2005). “Collapse analysis of masonry bridges taking into account
577 archfill interaction.” *Engineering Structures*, 27, 605–615.

578 Cazzani, A., Malagù, M., Stochino, F., and Turco, E. (2014a). “Constitutive models for strongly
579 curved beams in the frame of isogeometric analysis.” *accepted for publication on Mathematics
580 and Mechanics of Solids*.

581 Cazzani, A., Malagù, M., and Turco, E. (2014b). “Isogeometric analysis: a powerful numerical tool
582 for the elastic analysis of historical masonry arches.” *accepted for publication on Continuum
583 Mechanics and Thermodynamics*.

584 Cazzani, A., Malagù, M., and Turco, E. (2014c). “Isogeometric analysis of plane curved beams.”
585 *Mathematics and Mechanics of Solids*, DOI 10.1177/1081286514531265.

586 Charnes, A. and Greenberg, H. J. (1951). “Plastic collapse and linear programming.” *Bulletin of
587 the American Mathematical Society*, 57, 480–485.

588 CIRC2009. *Istruzioni per l’applicazione delle Nuove Norme Tecniche per le Costruzioni di cui
589 al D.M. 14 gennaio 2008*. Circolare n. 617 02/02/2009, Gazzetta Ufficiale della Repubblica
590 Italiana, (in Italian).

591 CNR2013. *Istruzioni per la Progettazione, l’Esecuzione ed il Controllo di Interventi di Consol-
592 idamento Statico mediante l’utilizzo di Compositi Fibrorinforzati*. DT200 R2013, Consiglio
593 Nazionale delle Ricerche, 2013 (in Italian).

594 Como, M. (2013). *Statics of historic masonry constructions*. Springer Verlag, Berlin-Heidelberg.

595 Cottrel, J. A., Hughes, T. J. R., and Reali, A. (2007). “Studied of refinement and continuity in
596 isogeometric structural analysis.” *Computer Methods in Applied Mechanics and Engineering*,

597 196, 4160–4183.

598 Cottrell, J. A., Hughes, T. J. R., and Bazilevs, Y. (2009). *Isogeometric Analysis: Toward Integration*
599 *of CAD and FEA*. Wiley, New York.

600 Cox, M. G. (1972). “The numerical evaluation of B-splines.” *Journal of the Institute of Mathemat-*
601 *ics and its Applications*, 10, 134–149.

602 Crisfield, M. G. (1997). *Non-linear finite element analysis of solids and structures*, Vol. 1 and 2.
603 Wiley, 2nd edition.

604 Cundall, P. A. and Strack, O. D. L. (1979). “A discrete numerical model for granular assemblies.”
605 *Geotechnique*, 29, 47–65.

606 de Boor, C. (1978). *A practical guide to splines*. Springer Verlag, New York, 1st edition.

607 Delbecq, J. M. (1980). “Analyse de la stabilité des voûtes en maçonnerie et en béton non armé par
608 le calcul á la rupture.” *Document interne SETRA*.

609 Farin, G. (2002). *Curves and Surfaces for CAGD: A Practical Guide*. Morgan Kaufmann Publish-
610 ers, San Francisco, 5th edition.

611 Ferris, M. C. and Tin-Loi, F. (2001). “Limit analysis of frictional block assemblies as a mathemat-
612 ical program with complementarity constraints.” *International Journal of Mechanical Sciences*,
613 43, 209–227.

614 Gelfi, P. (2008). “Arco 2008, <<http://dicata.ing.unibs.it/gelfi/software/>>.”

615 Gilbert, M. (2007). “Limit analysis applied to masonry arch bridges: state-of-the-art and recent de-
616 velopments.” *Proceedings of 5th International Conference on Arch Bridges*, Madeira, Portugal.

617 Gilbert, M. and Ahmed, H. M. (2004). “Developments to the RING masonry arch bridge analysis
618 software.” *Proceedings of 4th International Conference on Arch Bridges*, Barcelona, Spain.

619 Gilbert, M., Casapulla, C., and Ahmed, H. (2006). “Limit analysis of masonry block structures
620 with non-associative frictional joints using linear programming.” *Computers and structures*, 84,
621 873–887.

622 Gilbert, M. and Melbourne, C. (1994). “Rigid-block analysis of masonry structures.” *The structural*
623 *engineer*, 72, 356–361.

624 Gilbert, M., Nguyen, D., and Smith, C. (2007). “Computational limit analysis of soil-arch inter-
625 action in masonry arch bridges.” *Proceedings of 5th International Conference on Arch Bridges*,
626 Madeira, Portugal.

627 Gontier, C. and Vollmer, C. (1995). “A large displacement analysis of a beam using a CAD geo-
628 metric definition.” *Computers and Structures*, 57.

629 Greco, L. and Cuomo, M. (2013). “B-Spline interpolation of Kirchhoff-Love space rods.” *Com-*
630 *puter Methods in Applied Mechanics and Engineering*, 256, 251–269.

631 Greco, L. and Cuomo, M. (2014). “An implicit G1 multi patch B-spline interpolation for
632 KirchhoffLove space rods.” *Computer Methods in Applied Mechanics and Engineering*, 269,
633 173–197.

634 Hartley, P. J. and Judd, C. J. (1980). “Parametrization and shape of B-spline curves for CAD.”
635 *Computer-Aided Design*, 12, 235–238.

636 Heyman, J. (1966). “The stone skeleton.” *International Journal of Solids and Structures*, 2,
637 249–279.

638 Heyman, J. (1969). “The safety of masonry arches.” *International Journal of Mechanical Sciences*,
639 11, 363–385.

640 Heyman, J. (1982). *The masonry arch*. Ellis Horwood, Chichester.

641 Huerta, S. (2001). “Mechanics of masonry vaults: the equilibrium approach.” *Historical construc-*
642 *tions*, R.B. Lourenço and P. Roca , ed., Guimarães, 47–69.

643 Hughes, T. J. R., Cottrell, J. A., and Bazilevs, Y. (2005). “Isogeometric analysis: CAD, finite
644 elements, NURBS, exact geometry and mesh refinement.” *Computer Methods in Applied Me-*
645 *chanics and Engineering*, 194, 4135–4195.

646 Lee, E. T. Y. (1989). “Choosing nodes in parametric curve interpolation.” *Computer-Aided Design*,
647 21, 363–370.

648 LimitState Ltd. (2007). “LimitState:RING 3.0, <<http://www.limitstate.it/ring>>.

649 LimitState Ltd. (2011). *LimitState:RING User Manual Version 3.0*. Sheffield UK.

650 Lipshultz, M. (1969). *Theory and problems of differential geometry*. McGraw-Hill.

651 Livesley, R. K. A. (1978). "Limit analysis of structures formed from rigid blocks." *International*
652 *Journal for Numerical Methods in Engineering*, 12, 1853–1871.

653 Livesley, R. K. A. (1992). "A computational model for the limit analysis of three-dimensional
654 masonry structures." *Meccanica*, 27, 161–172.

655 Melbourne, C. and Gilbert, M. (1995). "The behaviour of multi-ring brickwork arch bridges." *The*
656 *Structural Engineer*, 73, 39–47.

657 Milani, E., Milani, G., and Tralli, A. (2008). "Limit analysis of masonry vaults by means of curved
658 shell finite elements and homogenization." *International Journal of Solids and Structures*, 45,
659 5258–5288.

660 Milani, G., Marzocchi, S., Minghini, F., and Tralli, A. (2014). "Seismic assessment of a masonry
661 tower in the region stricken by the 20-29 may 2012 emilia-romagna, italy, earthquake." *Proceed-*
662 *ings of the 9th International Masonry Conference*, R.B. Lourenço and P. Roca , ed., Guimarães,
663 Portugal.

664 Munjiza, A. (2004). *The combined finite-discrete element method*. Wiley, 1st edition.

665 NTC2008. *Norme tecniche per le costruzioni*. Decreto Ministeriale 14/01/2008, Gazzetta Ufficiale
666 della Repubblica Italiana, (in Italian).

667 Orduna, A. and Lourenço, P. (2003). "Cap model for limit analysis and strengthening of masonry
668 structures." *ASCE Journal of Structural Engineering*, 129, 1367–1375.

669 Piegl, L. and Tiller, W. (1997). *The NURBS book*. Springer Verlag, Berlin, 2nd edition.

670 Prenter, P. M. (1975). *Splines and variational methods*. Wiley, New York.

671 Roca, P., Cervera, M., G., G., and Pelà, L. (2007). "Structural analysis of masonry historical
672 constructions." *Engineering Structures*, 17, 299–325.

673 Sarkar, B. and Menq, C. H. (1991). "Smooth-surface approximation and reverse engineering."
674 *Computer-Aided Design*, 23, 623–628.

675 Tralli, A., Alessandri, C., and Milani, G. (2014). "Computational methods for masonry vaults: a
676 review of recent results." *The Open Journal of Civil Engineering*, 8, 272–287.

677 Vasconcelos, G. and Lourenço, P. B. (2006). "Assessment of the in-plane shear strength of stone

678 masonry walls by simplified models.” *Proceedings of the 5th International Conference Struc-*
679 *tural Analysis of Historical Constructions*, R.B. Lourenç, P. Roca, C. Modena, S. Agrawal, ed.,
680 New Dehli, India.

681 Vermeltoort, A. (2001). “Analysis and experiments of masonry arches.” *Proceedings of Historical*
682 *Constructions*, R.B. Lourenço and P. Roca , ed., Guimarães, Portugal, 489–498.

683

List of Tables

684	1	Maximum and mean errors on the approximation of the polycentric arch with poly-	
685		line and	30
686	2	Masonry mechanical properties and backfill density for examples in Sections 5. . .	31
687	3	Collapse load multipliers resulting from limit analysis of the arch analyzed in Sec-	
688		tion 5.3, belonging to Torre Fornasini (Poggio Renatico, Italy) groin vault, under	
689		different assumptions	32

n° of P_i	Polyline		NURBS	
	E_∞ [m]	E_2 [m]	E_∞ [m]	E_2 [m]
10	9.95e-2	6.61e-2	1.34e-2	1.64e-3
20	2.49e-2	1.66e-2	0.79e-2	3.73e-4
40	0.62e-2	4.15e-3	0.93e-3	2.74e-5

TABLE 1: Maximum and mean errors on the approximation of the polycentric arch with polyline and

NURBS representations.

Mechanical Properties	Example discussed in Section 5.2	Examples discussed in Sections 5.3 and 5.4
Masonry Young's modulus (E)	2800 MPa	1500 MPa
Masonry shear modulus (G)	860 MPa	500 MPa
Masonry mass density (ρ_m)	1800 kg/m ³	1800 kg/m ³
Masonry compressive strength (f_c)	6.0 MPa	2.4 Mpa
Backfill mass density (ρ_b)	1600 kg/m ³	1600 kg/m ³

TABLE 2: Masonry mechanical properties and backfill density for examples in Sections 5.

FRP reinforcement	Arch Configuration	Collapse Load Multiplier λ
no	no backfill and unlimited masonry compressive strength	-
	backfill and unlimited masonry compressive strength	1.43
	backfill and limited masonry compressive strength	0.86
	backfill, unlimited masonry compressive strength and limited friction between blocks ($\mu = 0.3$)	1.43
	backfill, unlimited masonry compressive strength and limited friction between blocks ($\mu = 0.275$)	1.02
yes	backfill and unlimited masonry compressive strength	5.94
	backfill and limited masonry compressive strength	3.44

TABLE 3: Collapse load multipliers resulting from limit analysis of the arch analyzed in Section 5.3, belonging to Torre Fornasini (Poggio Renatico, Italy) groin vault, under different assumptions

690
691
692
693
694
695
696
697
698
699
700
701
702
703
704
705
706
707
708
709
710
711

List of Figures

- 1 Examples of historical arched structures: (a) three-centered masonry arch bridge in Llanelltyd, Wales (image courtesy of Bill Harvey) and (b) Porta Asinaria rounded stone voussoirs arch in Rome, Italy (image by authors). Both arches cannot be accurately modeled with polyline geometries. 35
- 2 Polycentric arch (solid circles denote the interpolating points P_i) 36
- 3 Reference system $O(x, y)$ and local reference system $O'(t', n')$ 37
- 4 Schematic representation of the segmental masonry test-arch used in (Vermeltfoort 2001): geometry and loading conditions. 38
- 5 (a) Failure mechanism experimentally obtained from (Vermeltfoort 2001). (b) Numerical failure mechanism (dashed lines) and thrust line at collapse (solid line) computed with ArchNURBS. Experimental failure photo is reported with the sole aim of showing the capabilities of the computational tool ArchNURBS (reprinted from (Vermeltfoort 2001), with permission.) 39
- 6 Thrust lines for the example arch computed with (a) quadrangular voussoirs (LimitState:RING 3.0[®]) and (b) rounded voussoirs (ArchNURBS) models. Corresponding collapse load multipliers λ are equal to 8.9 and 9.8, respectively. 40
- 7 Three-centered arch analyzed with ArchNURBS: thrust line (solid line) obtained without backfill (a) and with backfill (b). The collapse load multipliers corresponding to these configurations are 0.78 and 21.62, respectively. 41
- 8 (a) External view and (b) first story masonry groin vault of *Torre Fornasini* in Poggio Renatico, Italy (image by authors). 42

712 9 A masonry arch from *Torre Fornasini* in Poggio Renatico, (Ferrara, Italy) and
713 represented in (a) has been modeled within ArchNURBS. The thrust line (solid
714 line) and the position of the hinges (solid circles) at collapse are illustrated in (b).
715 Moreover, the solution of the limit analysis has been studied by considering (c) the
716 FRP reinforcement indicated with a solid line at the extrados (solid squares denote
717 the FRP delamination points) and (d) sliding between blocks (with $\mu = 0.275$). . . 43



(a)



(b)

FIG. 1: Examples of historical arched structures: (a) three-centered masonry arch bridge in Llanelltyd, Wales (image courtesy of Bill Harvey) and (b) Porta Asinaria rounded stone voussoirs arch in Rome, Italy (image by authors). Both arches cannot be accurately modeled with polyline geometries.

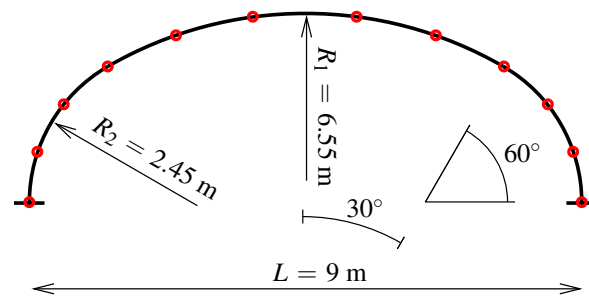


FIG. 2: Polycentric arch (solid circles denote the interpolating points P_i)

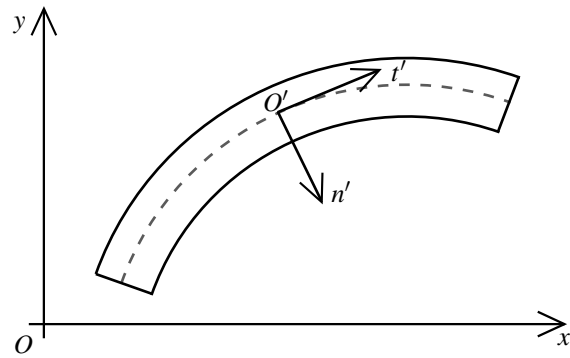


FIG. 3: Reference system $O(x, y)$ and local reference system $O'(t', n')$

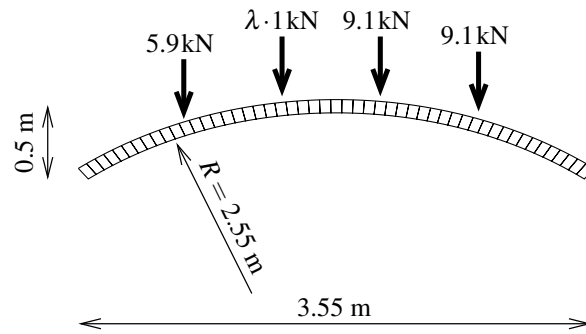
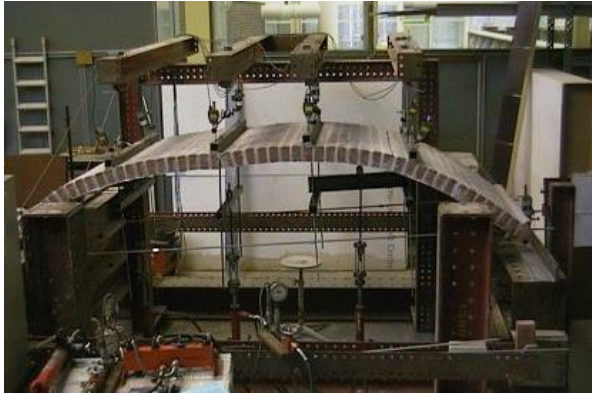
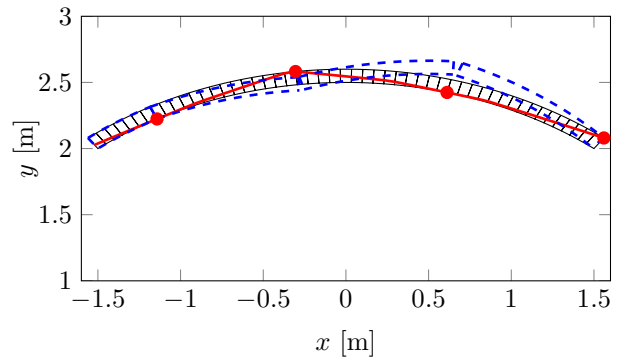


FIG. 4: Schematic representation of the segmental masonry test-arch used in (Vermeltfoort 2001): geometry and loading conditions.



(a)



(b)

FIG. 5: (a) Failure mechanism experimentally obtained from (Vermeltoort 2001). (b) Numerical failure mechanism (dashed lines) and thrust line at collapse (solid line) computed with ArchNURBS. Experimental failure photo is reported with the sole aim of showing the capabilities of the computational tool ArchNURBS (reprinted from (Vermeltoort 2001), with permission.)

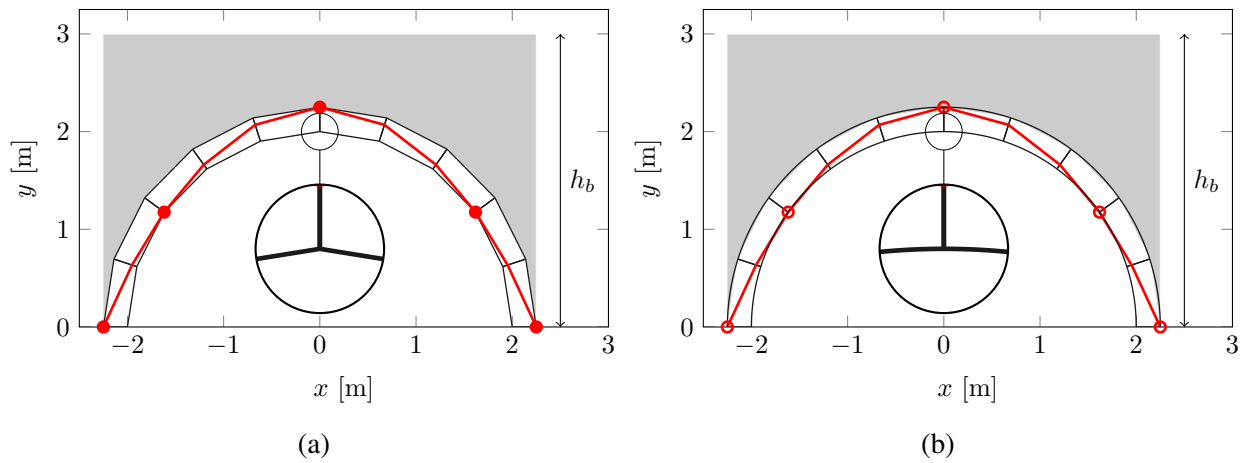


FIG. 6: Thrust lines for the example arch computed with (a) quadrangular voussoirs (Limit-State:RING 3.0[®]) and (b) rounded voussoirs (ArchNURBS) models. Corresponding collapse load multipliers λ are equal to 8.9 and 9.8, respectively.

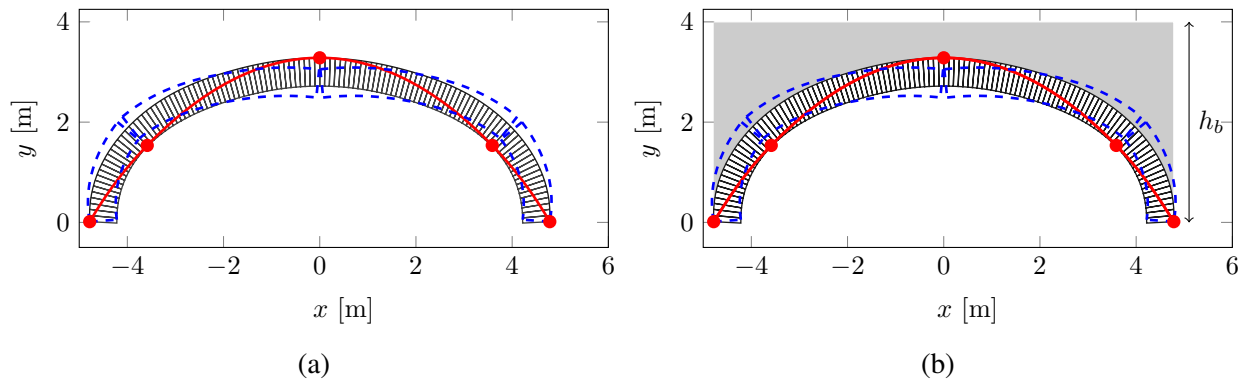


FIG. 7: Three-centered arch analyzed with ArchNURBS: thrust line (solid line) obtained without backfill (a) and with backfill (b). The collapse load multipliers corresponding to these configurations are 0.78 and 21.62, respectively.



(a)



(b)

FIG. 8: (a) External view and (b) first story masonry groin vault of *Torre Fornasini* in Poggio Renatico, Italy (image by authors).

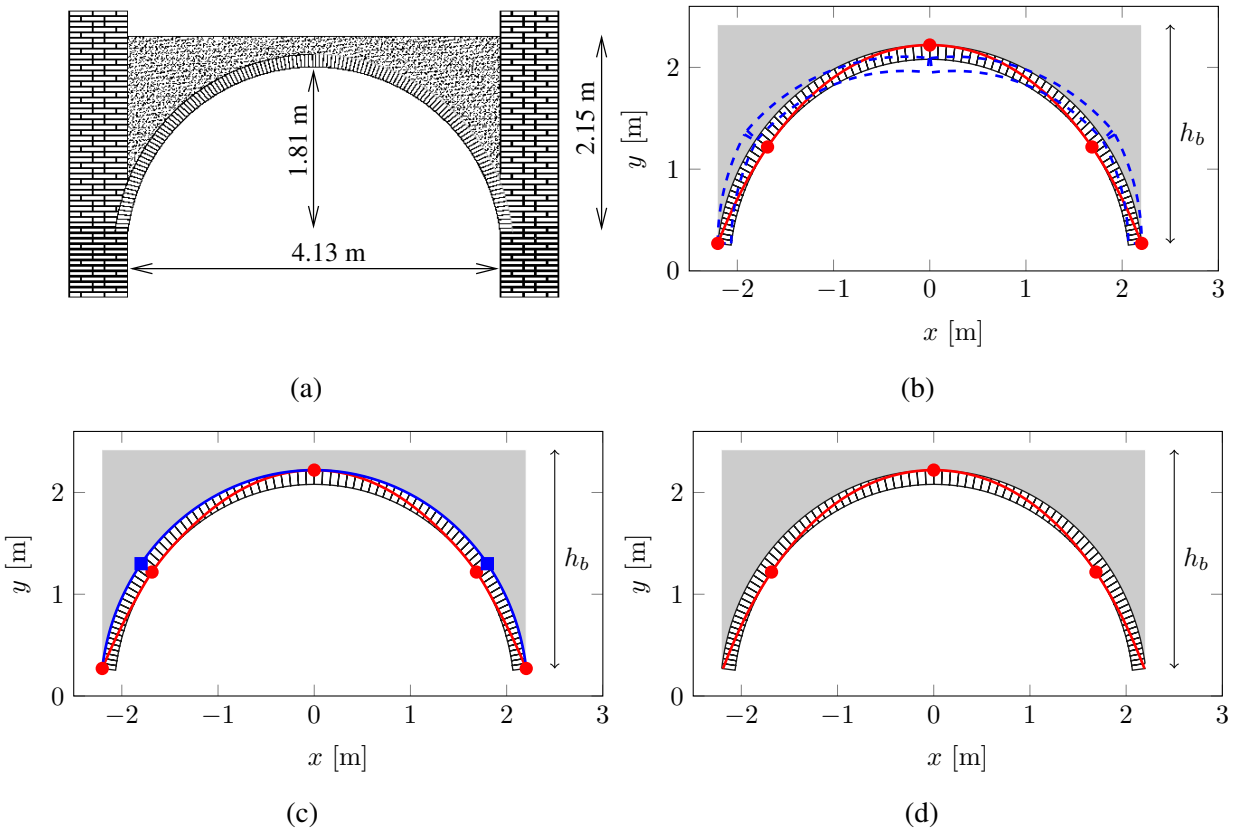


FIG. 9: A masonry arch from *Torre Fornasini* in Poggio Renatico, (Ferrara, Italy) and represented in (a) has been modeled within ArchNURBS. The thrust line (solid line) and the position of the hinges (solid circles) at collapse are illustrated in (b). Moreover, the solution of the limit analysis has been studied by considering (c) the FRP reinforcement indicated with a solid line at the extrados (solid squares denote the FRP delamination points) and (d) sliding between blocks (with $\mu = 0.275$).